Pulsed Fission-Fusion Propulsion System

Robert B. Adams, Ph.D.
ER24/Propulsion Research and Technology Branch
George C. Marshall Space Flight Center
National Aeronautics and Space Administration

Jason Cassibry, Ph.D.
Propulsion Research Center
Department of Mechanical and Aerospace Engineering
University of Alabama in Huntsville

NIAC
NASA Innovative Advanced Concepts

Challenges and Underlying Physics of Nuclear Processes

Fission and Fusion Energy Release

- **Mass Defect = Mass of free nucleons – mass of assembled nucleus**
  - Nuclear force (residual strong force) stronger than electrostatic
- **Nuclear Binding Energy**
  - $\frac{E}{A} = \frac{\Delta m}{A} c^2$
- **Fusion**
  - Energy release by combining nuclei
- **Fission**
  - Energy release by splitting nuclei

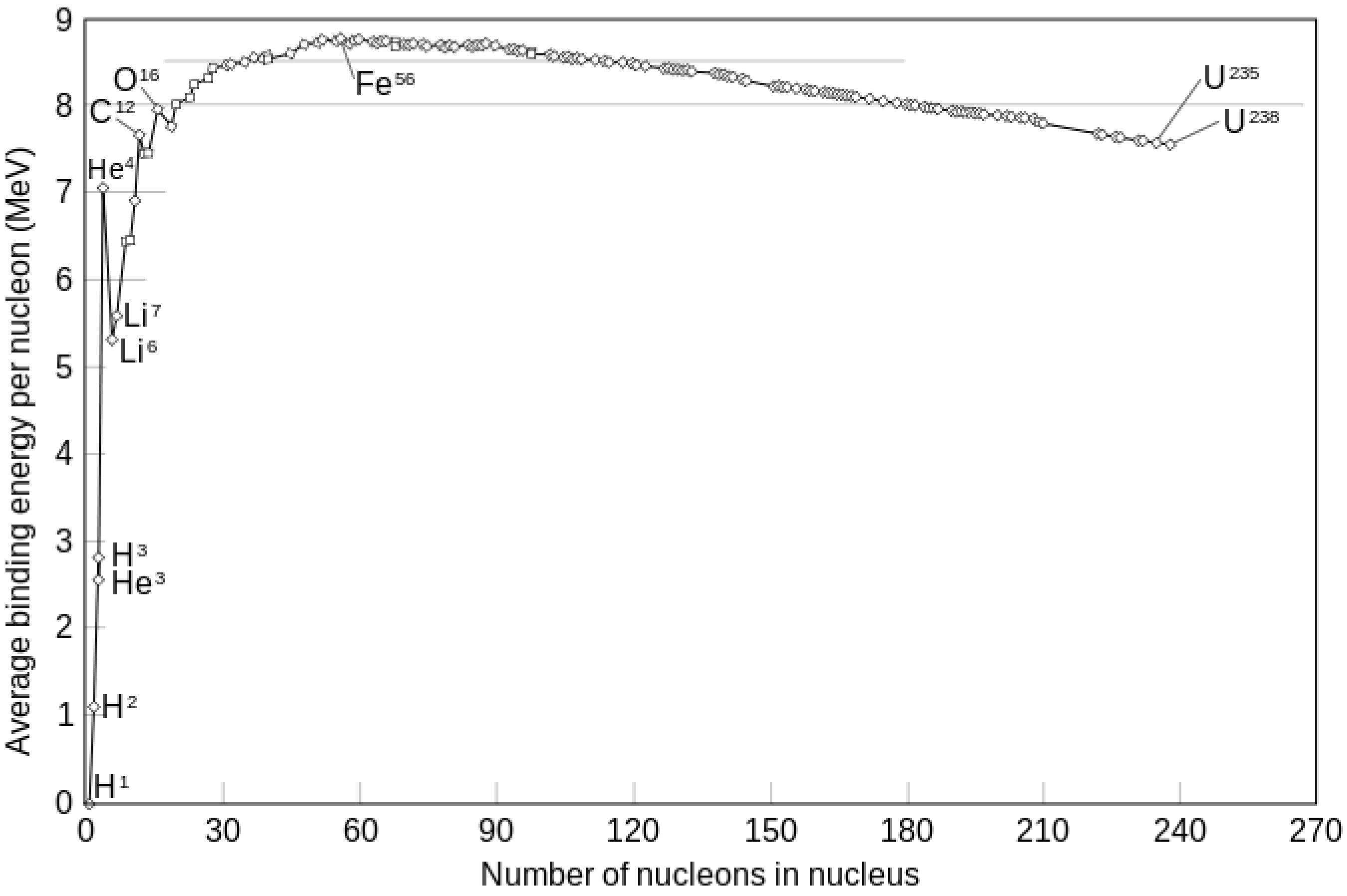

http://en.wikipedia.org/wiki/Nuclear_binding_energy

Fission and Fusion Reaction Space

Marshall Space Flight Center

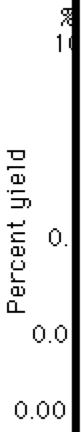

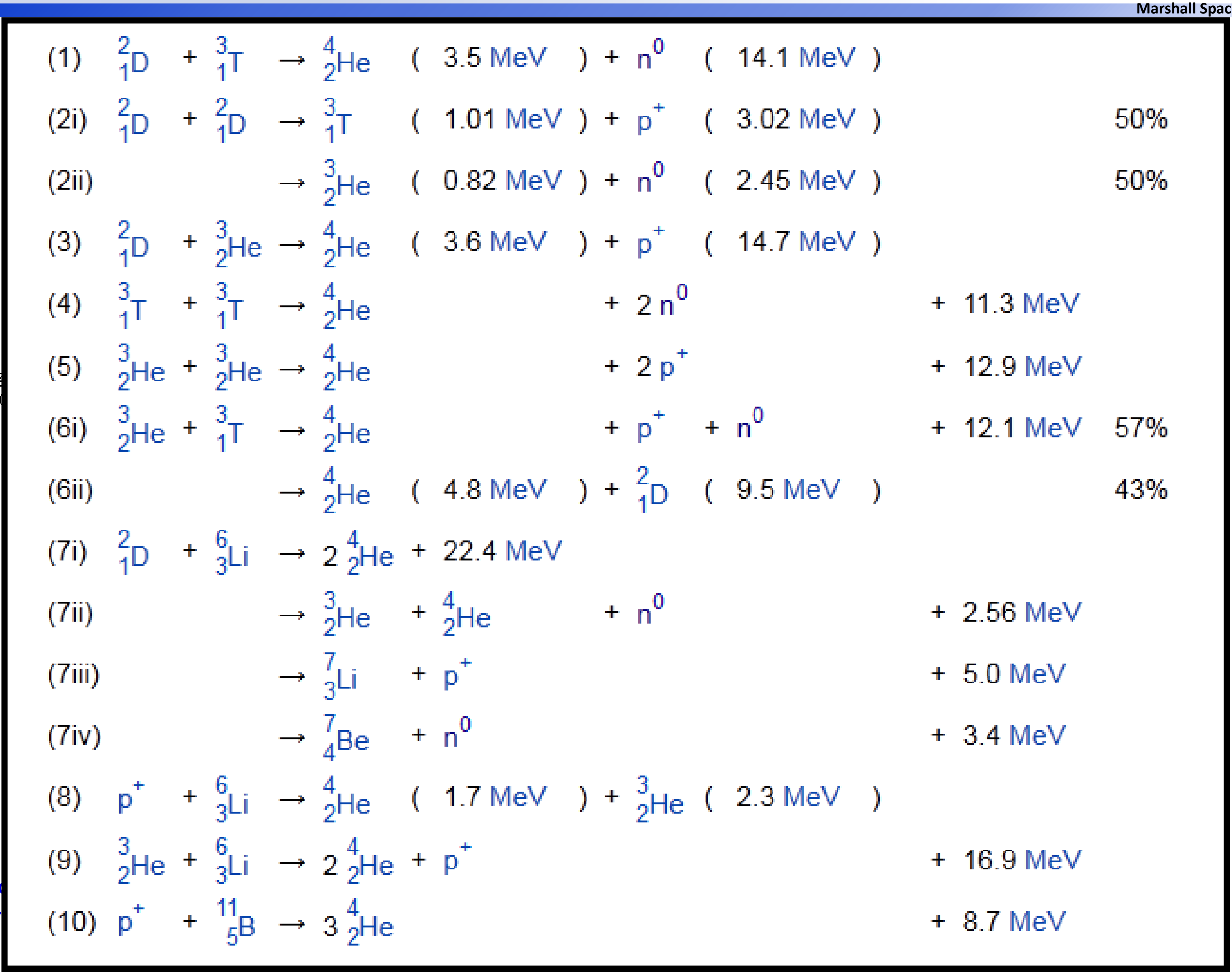

(1) ${}^{2}_{1}\mathrm{D} + {}^{3}_{1}\mathrm{T} \rightarrow {}^{4}_{2}\mathrm{He}$ (3.5 MeV) + n^{0} (14.1 MeV)

(2i) ${}^{2}_{1}\mathrm{D} + {}^{2}_{1}\mathrm{D} \rightarrow {}^{3}_{1}\mathrm{T}$ (1.01 MeV) + p^{+} (3.02 MeV) 50%

(2ii) $\rightarrow {}^{3}_{2}\mathrm{He}$ (0.82 MeV) + n^{0} (2.45 MeV) 50%

(3) ${}^{2}_{1}\mathrm{D} + {}^{3}_{2}\mathrm{He} \rightarrow {}^{4}_{2}\mathrm{He}$ (3.6 MeV) + p^{+} (14.7 MeV)

(4) ${}^{3}_{1}\mathrm{T} + {}^{3}_{1}\mathrm{T} \rightarrow {}^{4}_{2}\mathrm{He} + 2\,n^{0}$ + 11.3 MeV

(5) ${}^{3}_{2}\mathrm{He} + {}^{3}_{2}\mathrm{He} \rightarrow {}^{4}_{2}\mathrm{He} + 2\,p^{+}$ + 12.9 MeV

(6i) ${}^{3}_{2}\mathrm{He} + {}^{3}_{1}\mathrm{T} \rightarrow {}^{4}_{2}\mathrm{He} + p^{+} + n^{0}$ + 12.1 MeV 57%

(6ii) $\rightarrow {}^{4}_{2}\mathrm{He}$ (4.8 MeV) + ${}^{2}_{1}\mathrm{D}$ (9.5 MeV) 43%

(7i) ${}^{2}_{1}\mathrm{D} + {}^{6}_{3}\mathrm{Li} \rightarrow 2\,{}^{4}_{2}\mathrm{He}$ + 22.4 MeV

(7ii) $\rightarrow {}^{3}_{2}\mathrm{He} + {}^{4}_{2}\mathrm{He} + n^{0}$ + 2.56 MeV

(7iii) $\rightarrow {}^{7}_{3}\mathrm{Li} + p^{+}$ + 5.0 MeV

(7iv) $\rightarrow {}^{7}_{4}\mathrm{Be} + n^{0}$ + 3.4 MeV

(8) $p^{+} + {}^{6}_{3}\mathrm{Li} \rightarrow {}^{4}_{2}\mathrm{He}$ (1.7 MeV) + ${}^{3}_{2}\mathrm{He}$ (2.3 MeV)

(9) ${}^{3}_{2}\mathrm{He} + {}^{6}_{3}\mathrm{Li} \rightarrow 2\,{}^{4}_{2}\mathrm{He} + p^{+}$ + 16.9 MeV

(10) $p^{+} + {}^{11}_{5}\mathrm{B} \rightarrow 3\,{}^{4}_{2}\mathrm{He}$ + 8.7 MeV

http n/
roje
Pow
http

Ignition Requirements

Fission

- Criticality is a function of
  - fission cross section
  - Number density
  - And geometry
- Neutrons must balance
  - Lost outside reactor
  - Absorbed through photon capture
  - Fission events

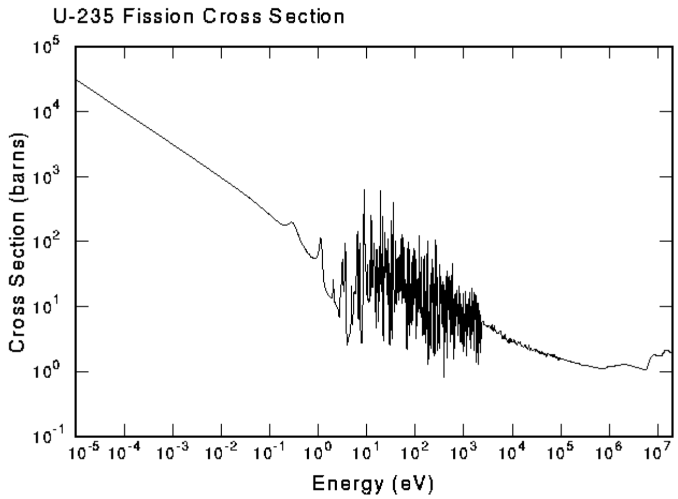

http://t2.lanl.gov/nis/tour/sch002.html

Fusion

- Breakeven is a function of
  - Fusion cross section
  - temperature distribution
  - density
- Lawson Criterion
  - $n_e \tau_E \geq \frac{12 k_B}{E_{ch}} \frac{T}{\langle \sigma v \rangle}$

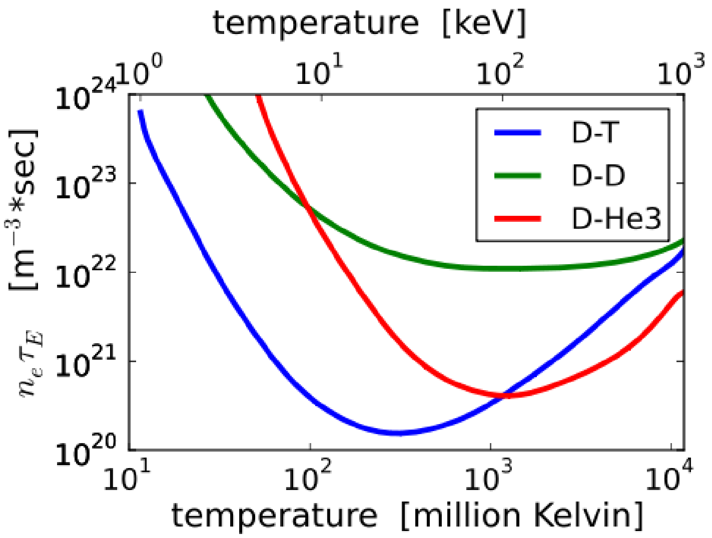

http://en.wikipedia.org/wiki/Lawson_criterion

Fusion Confinement Parameter Space

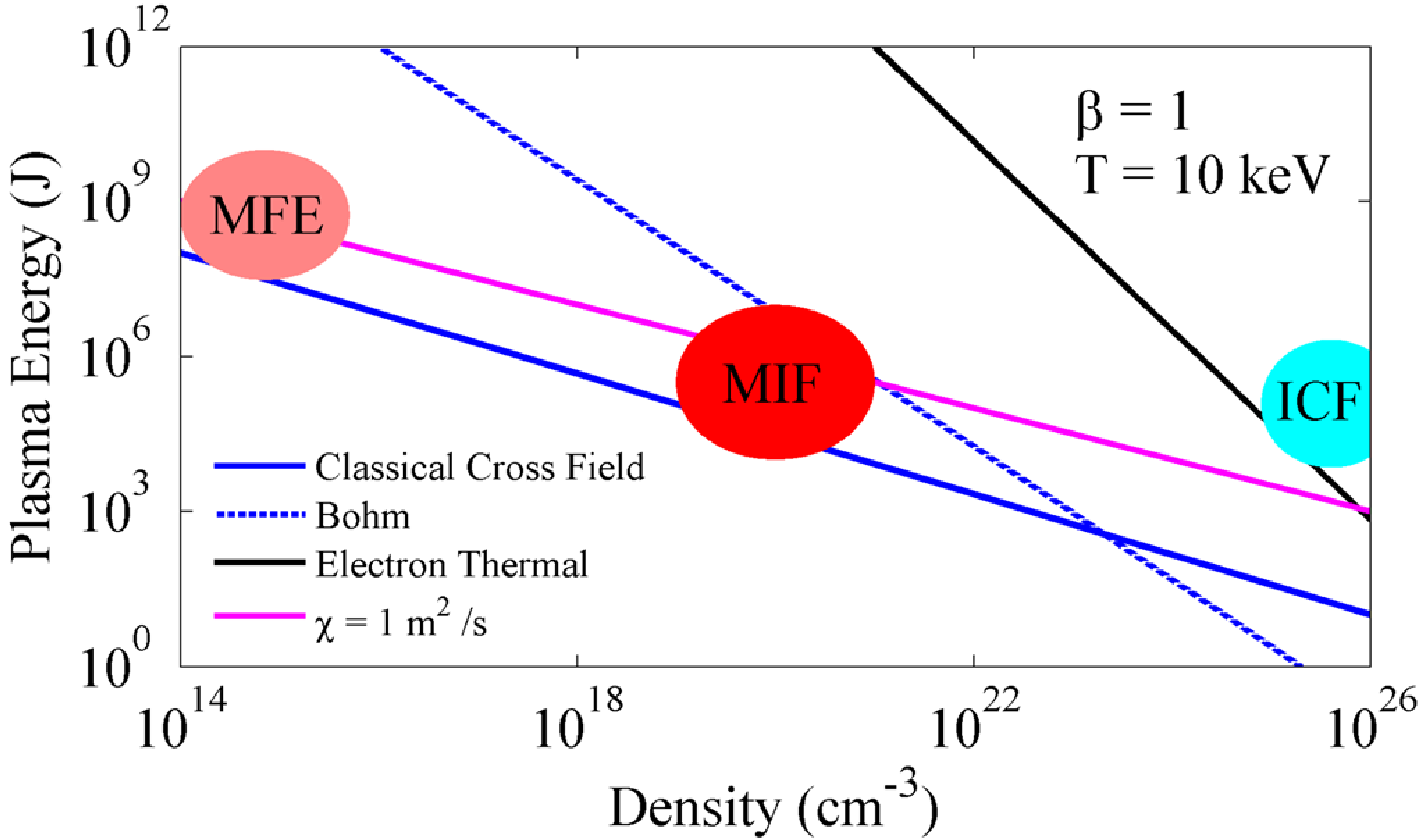

Benefits of MIF Parameter Space

- Fusion reactivity scales with n^2
- Magnetic field suppresses thermal conduction losses, reducing driver power
- Reactor volume much smaller than MFE
- These effects lead to potentially much lower cost, smaller fusion reactor, as suggested by Lindemuth and Siemon, Am. J. Phys., 77(5), May 2009

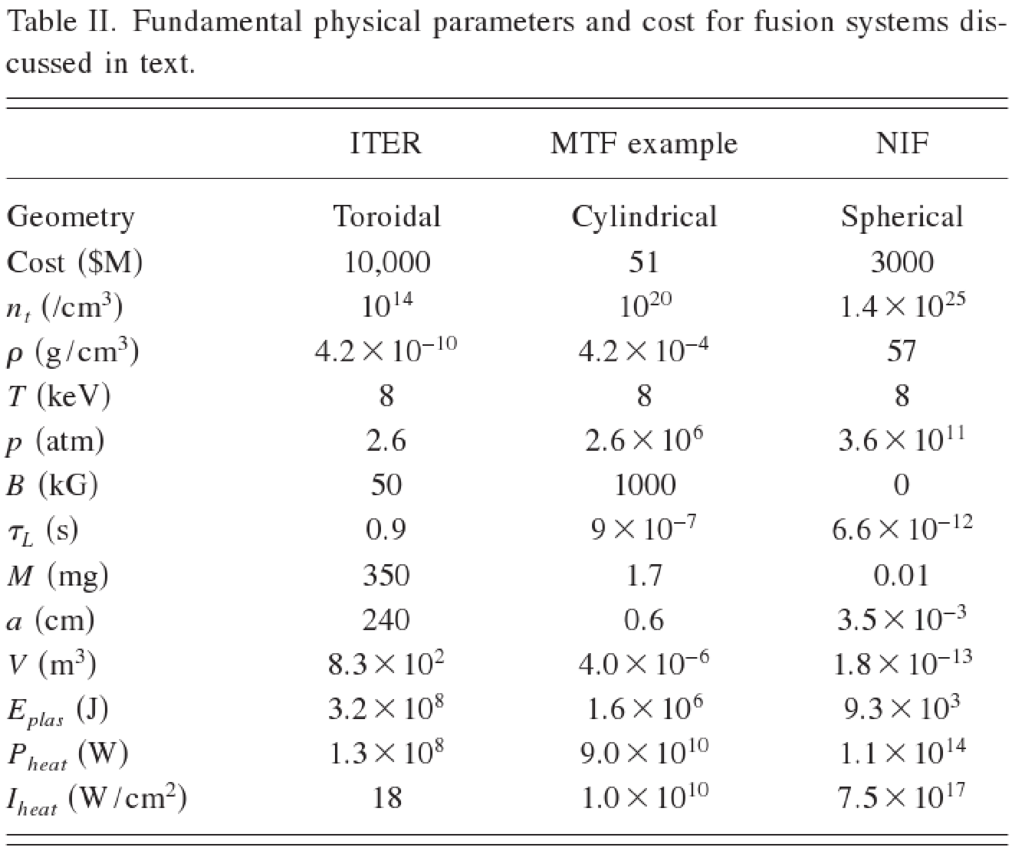

Table II. Fundamental physical parameters and cost for fusion systems discussed in text.

	ITER	MTF example	NIF
Geometry	Toroidal	Cylindrical	Spherical
Cost ($M)	10,000	51	3000
n_t (/cm^3)	10^{14}	10^{20}	1.4×10^{25}
ρ (g/cm^3)	4.2×10^{-10}	4.2×10^{-4}	57
T (keV)	8	8	8
p (atm)	2.6	2.6×10^{6}	3.6×10^{11}
B (kG)	50	1000	0
τ_L (s)	0.9	9×10^{-7}	6.6×10^{-12}
M (mg)	350	1.7	0.01
a (cm)	240	0.6	3.5×10^{-3}
V (m^3)	8.3×10^{2}	4.0×10^{-6}	1.8×10^{-13}
E_{plas} (J)	3.2×10^{8}	1.6×10^{6}	9.3×10^{3}
P_{heat} (W)	1.3×10^{8}	9.0×10^{10}	1.1×10^{14}
I_{heat} (W/cm^2)	18	1.0×10^{10}	7.5×10^{17}

PuFF Concept

Introduction to PuFF

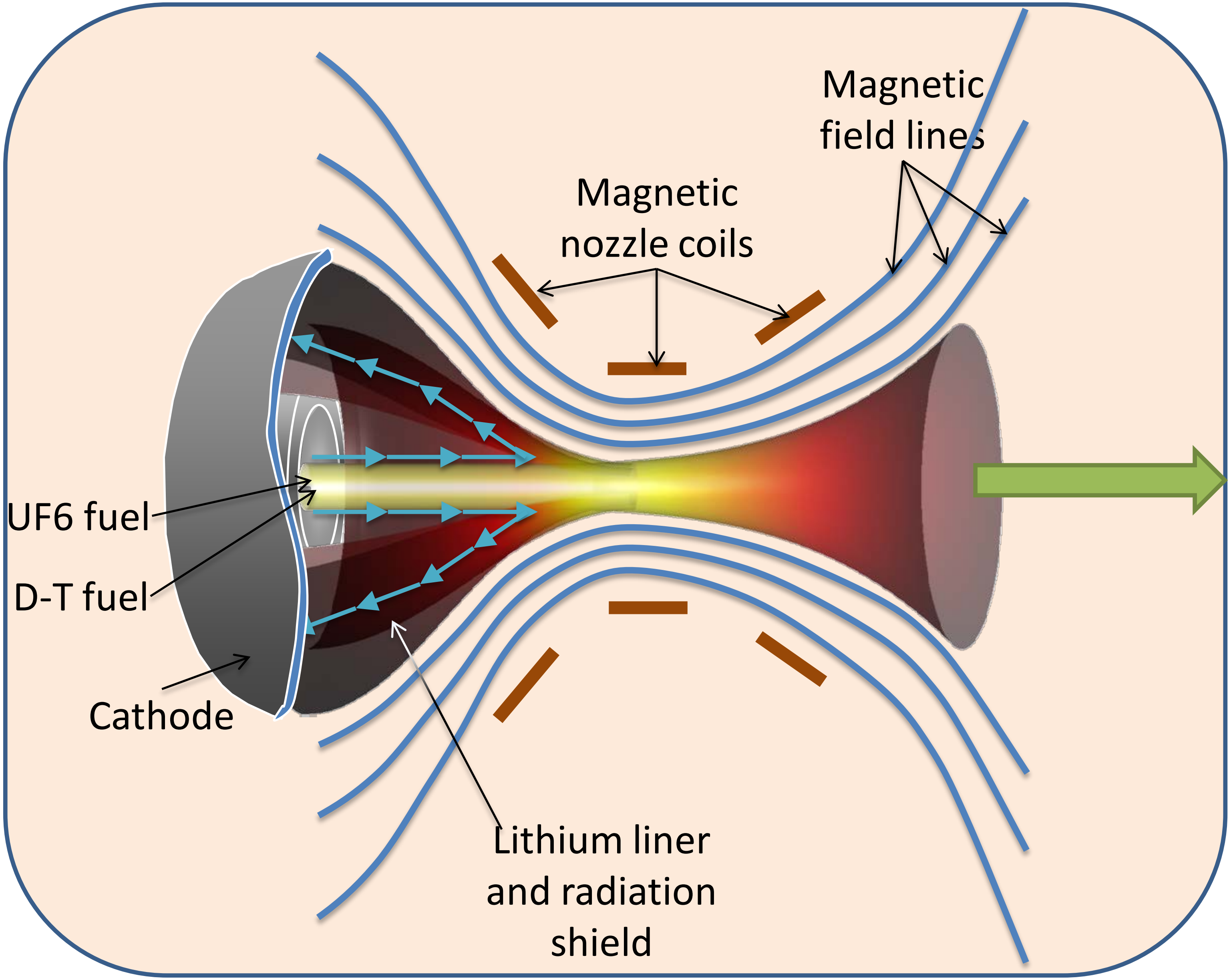

Operation of a Z Pinch

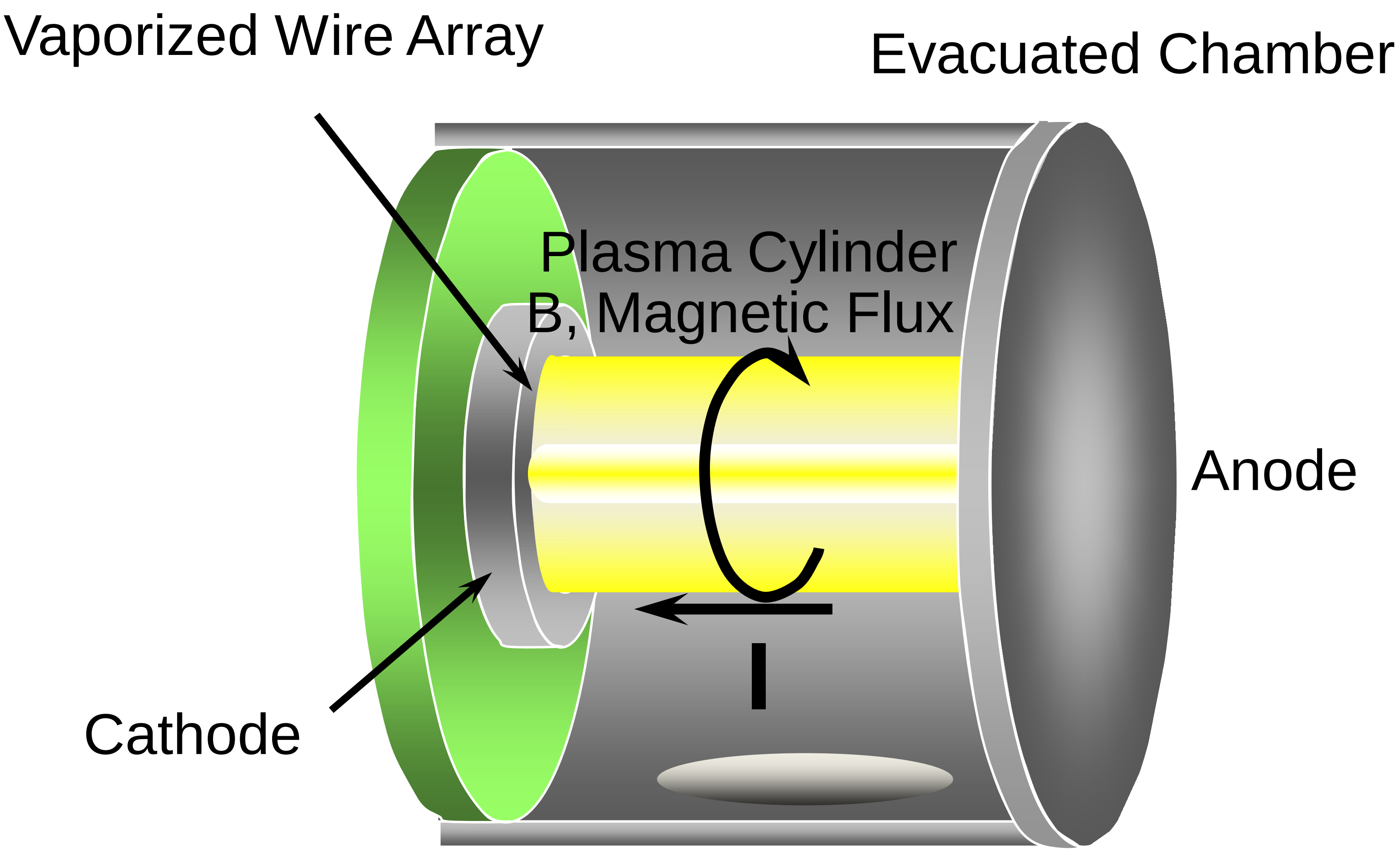

Fission-Fusion Energy Balance

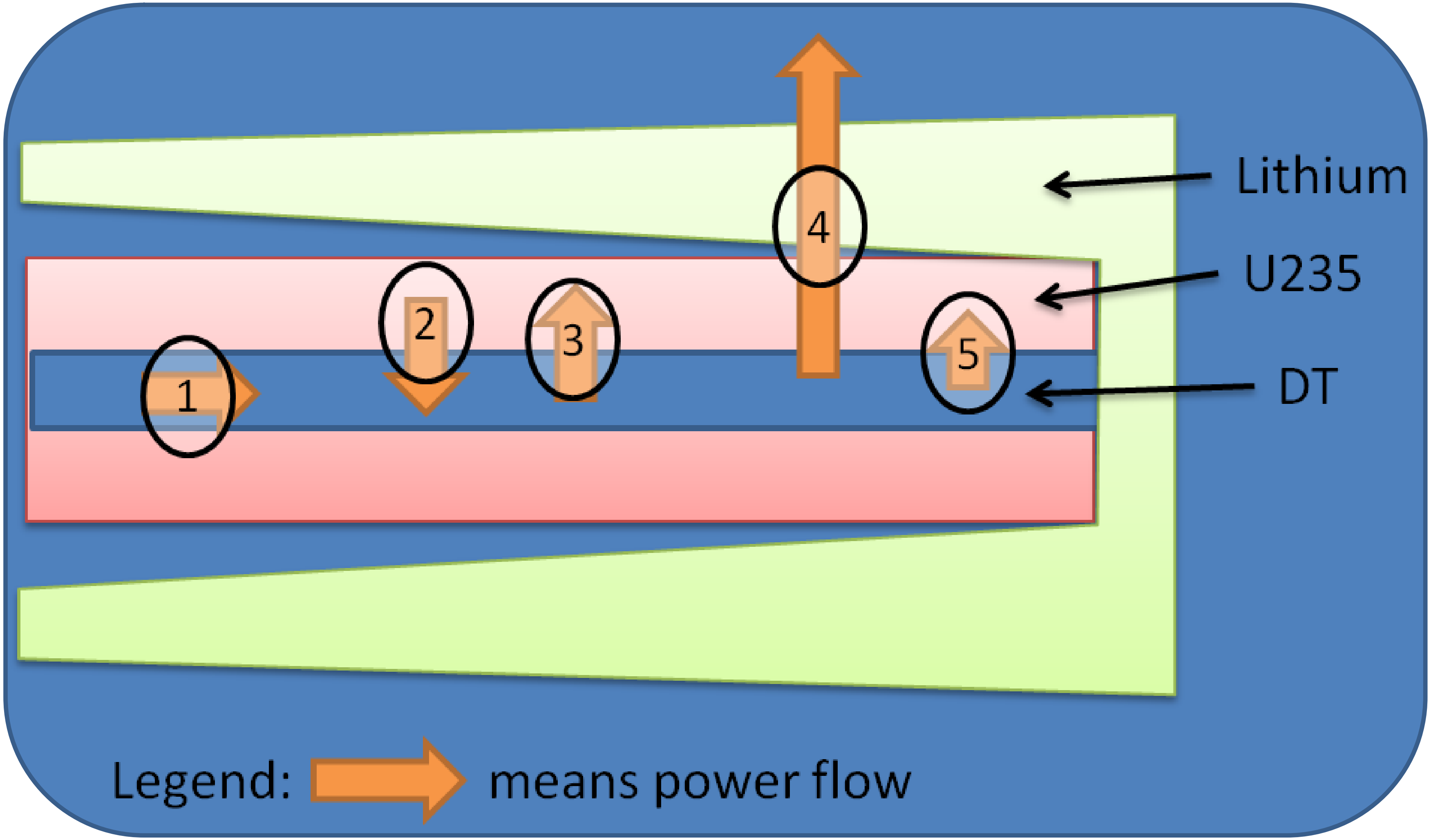

Research Status

Heating Mechanisms Included in Model

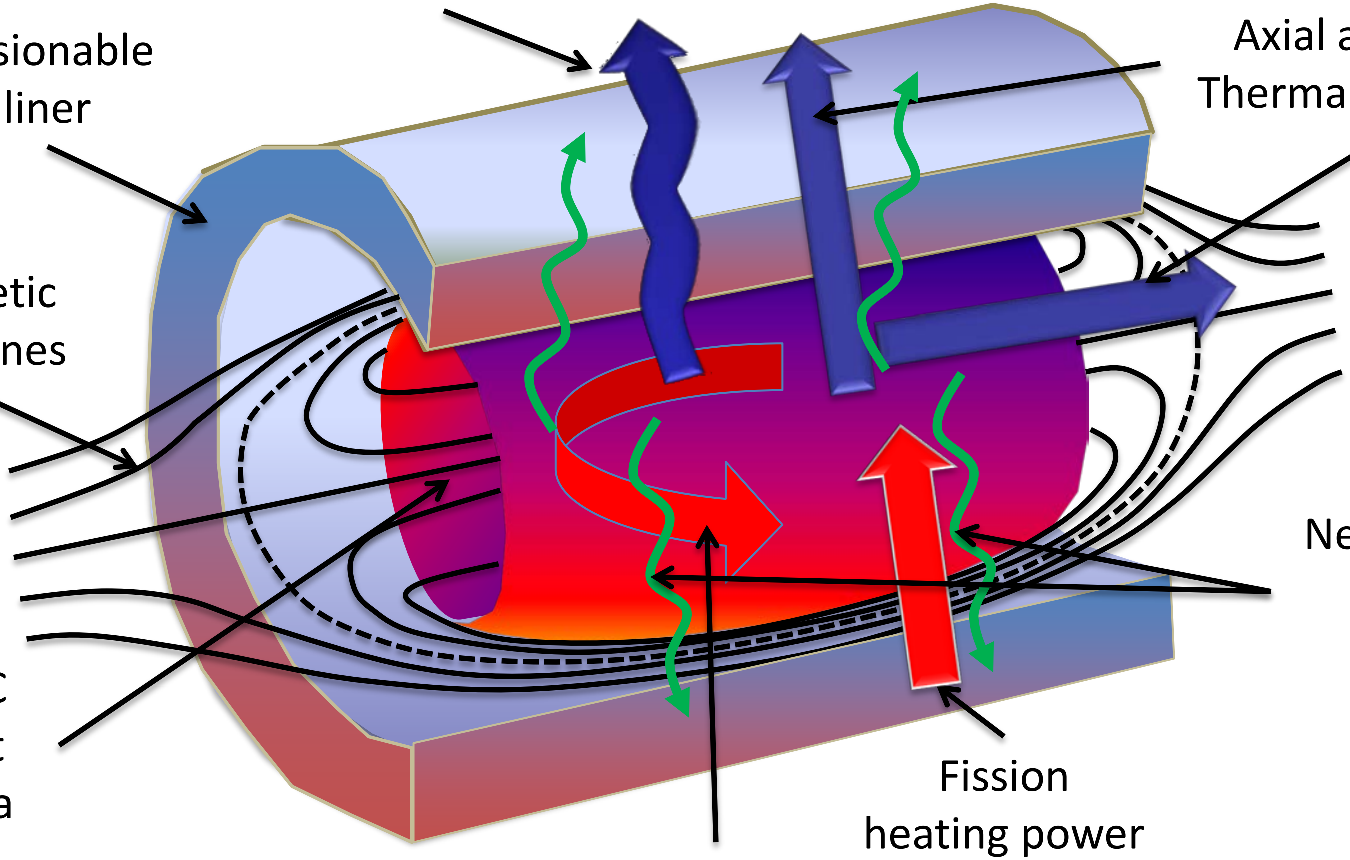

Bremmstrahlung and Cyclotron Radiation

Fissionable liner

Axial and Radial Thermal conduction

Magnetic Field Lines

Neutron induced Fast fission reactions

DT FRC Target Plasma

Fission heating power

Fusion heating power

Fission- Fusion Power Balance

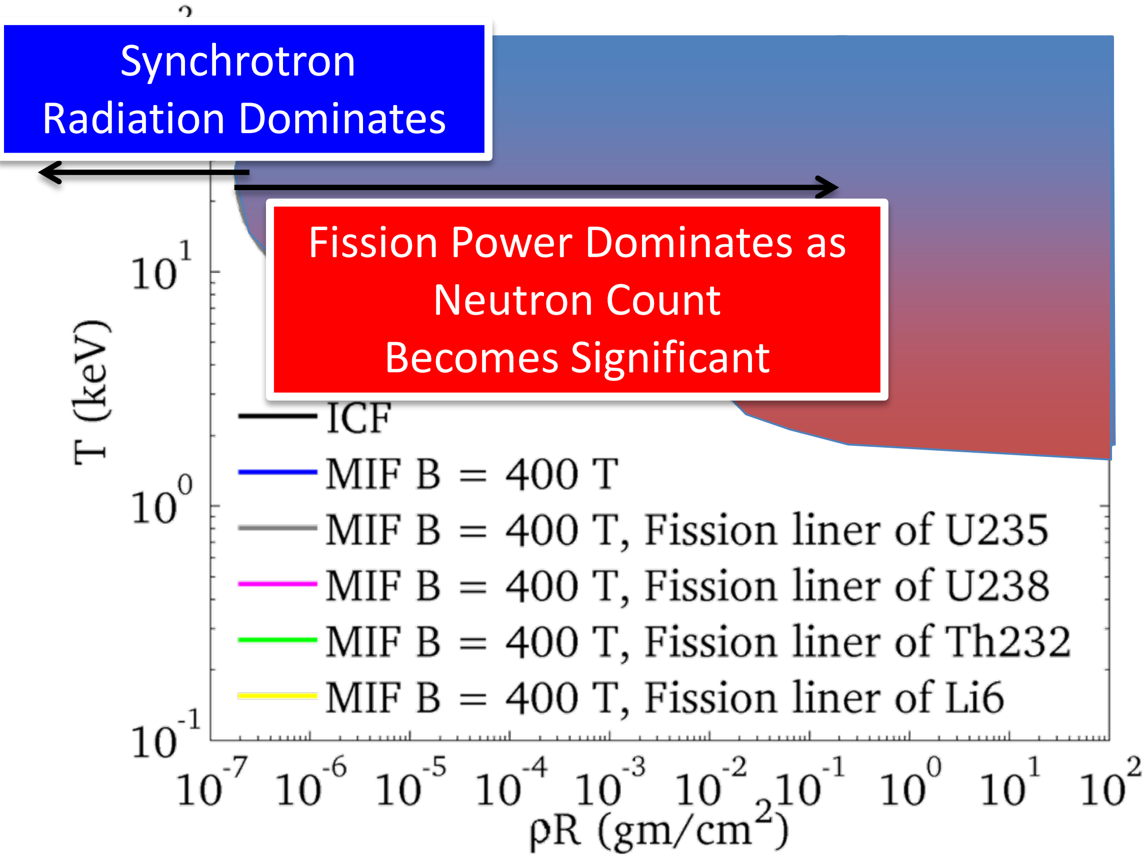

Synchrotron Radiation Dominates

Fission Power Dominates as Neutron Count Becomes Significant

- Parameter space for ignition
- Greatly broadened with embedded magnetic field
- Marginally improved with ^{6}Li and thorium liners
- Significantly enhanced with uranium liners (^{235}U and ^{238}U)

Our Approach: Solve Maxwell's Equations Coupled to Multifluid (Ions, Electrons, Neutrals) Equations of Motion

Maxwell's Equations

- Solve with Smooth Particle Electromagnetic Variant of Finite-Difference Time Domain (FDTD) method
- FDTD well documented, highly accurate grid-based method for analyzing the time evolution of electric and magnetic fields
- Can interpolate charged fluid particles to grid to model conductivity or charge and current density

Multifluid Equations of Motions

- Solve with Smooth Particle Hydrodynamics (SPH)
- Gridless Lagrangian technique
- Vacuum/plasma boundary well defined
- Leverage same engine as Maxwell Equation Solver

Both methods yield to 'vectorized' coding, making multiprocessor (parallel) computing easy

Equations of motion (completed)

$$\frac{\partial}{\partial t} n_e + \nabla \cdot \mathbf{u}_e = 0$$

$$\frac{\partial}{\partial t} n_i + \nabla \cdot \mathbf{u}_i = 0$$

$$n_e m_e \frac{\partial}{\partial t} \mathbf{u}_e + \nabla p_e + e n_e \left(\mathbf{E} + \mathbf{u}_e \times \mathbf{B} \right) = -$$

$$n_i m_i \frac{\partial}{\partial t} \mathbf{u}_i + \nabla p_i - Z e n_i \left(\mathbf{E} + \mathbf{u}_i \times \mathbf{B} \right) =$$

$$\frac{3}{2} n_e \frac{\partial}{\partial t} k T_e + p_e \nabla \cdot \mathbf{u}_e = -\pi_e : \nabla \mathbf{u}_e - \nabla \mathbf{h}_e - \left(\mathbf{u}_e - \mathbf{u}_i \right) \cdot \mathbf{R}_e - Q_i$$

$$\frac{3}{2} n_i \frac{\partial}{\partial t} k T_i + p_i \nabla \cdot \mathbf{u}_i = -\pi_i : \nabla \mathbf{u}_i - \nabla \mathbf{h}_i - Q_i$$

Transport effects,
which can be based
on nonequilibrium
distribution functions
(kappa and power law)

$$\mathbf{R}_\alpha \equiv \int m_\alpha \mathbf{w} \sum_\beta C_{\alpha\beta} \, d\mathbf{w}$$

$$\mathbf{R}_\alpha \approx -\sum_\beta m_\alpha n_\alpha \left(\mathbf{V}_\alpha - \mathbf{V}_\beta \right) \langle \nu_{\alpha\beta} \rangle$$

$$p_\alpha \equiv \frac{1}{3} n_\alpha m_\alpha \langle w^2 \rangle$$

$$\pi_i \equiv n_\alpha m_\alpha \langle \mathbf{w}\mathbf{w} \rangle - p_\alpha \mathbf{I}$$

$$h_\alpha \equiv \frac{1}{2} n_\alpha m_\alpha \langle w^2 \mathbf{w} \rangle$$

$$Q_\alpha \equiv \int \frac{1}{2} m_\alpha w_\alpha^2 \sum_\beta C_{\alpha\beta} \, d\mathbf{w}$$

Initial Pulsed Nozzle Model

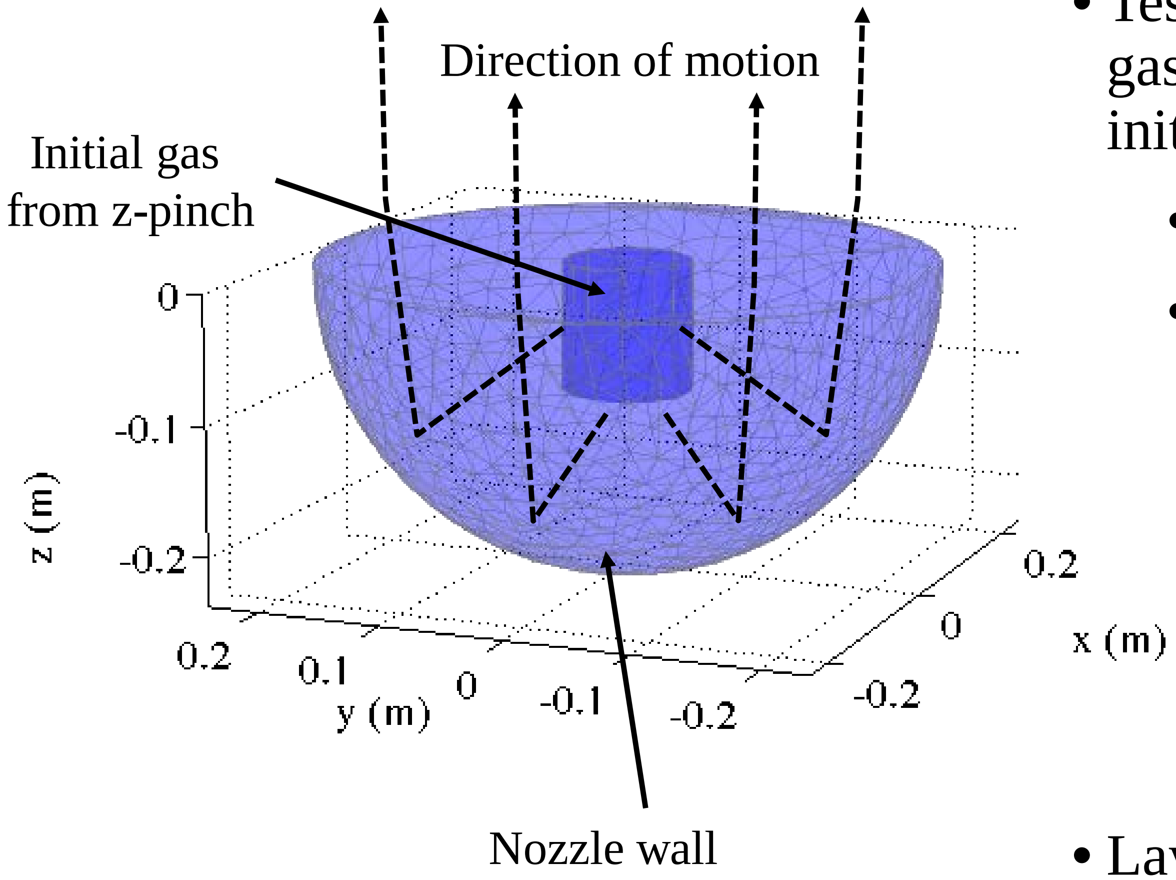

- Test thermal expansion of gas nozzle with various initial conditions
  - Nozzle geometry
  - Gas
    - Temperature
    - Density
    - Radius
    - Length
    - Composition
- Lays ground work and expectations for magnetic nozzle

Preliminary results

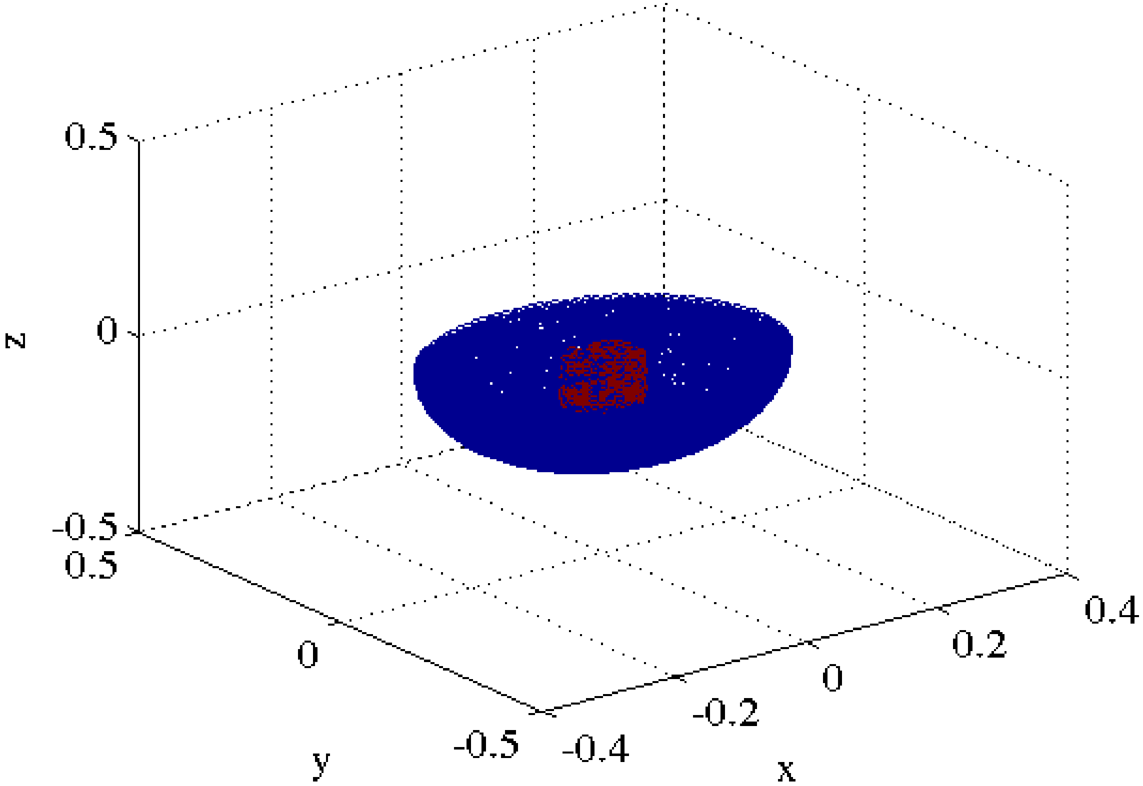

Preliminary results

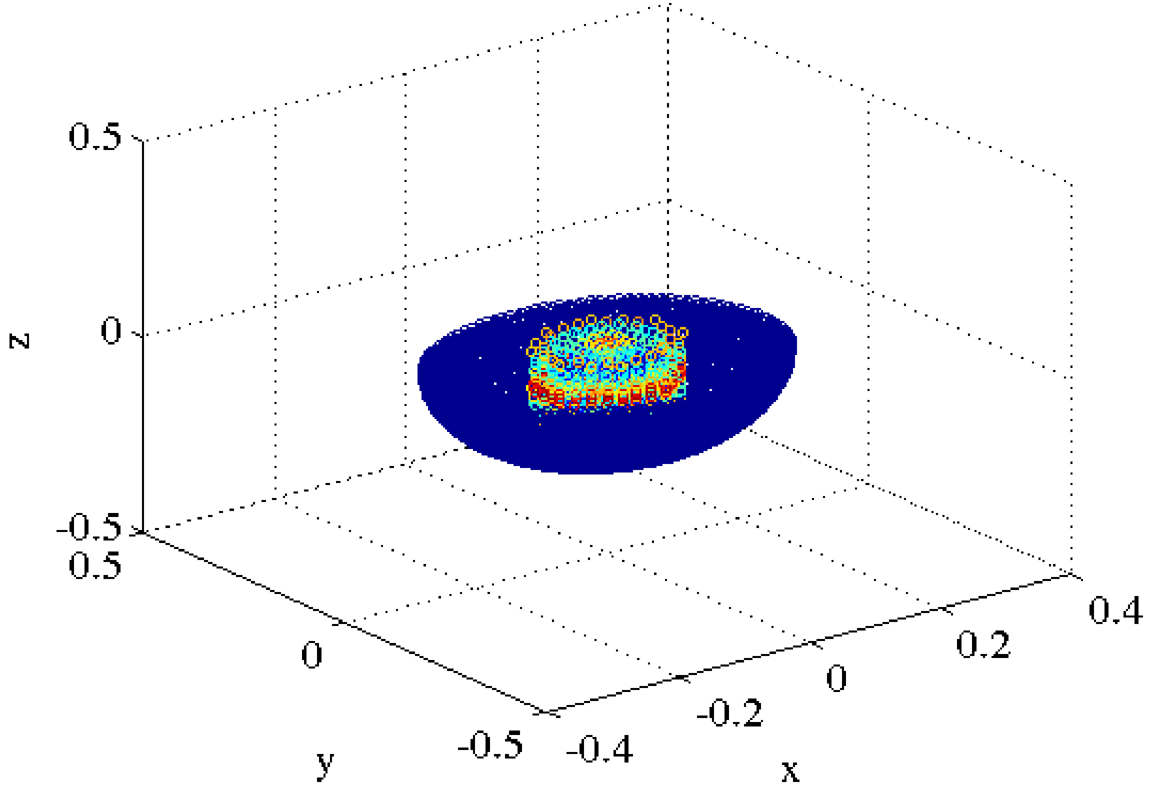

Preliminary results

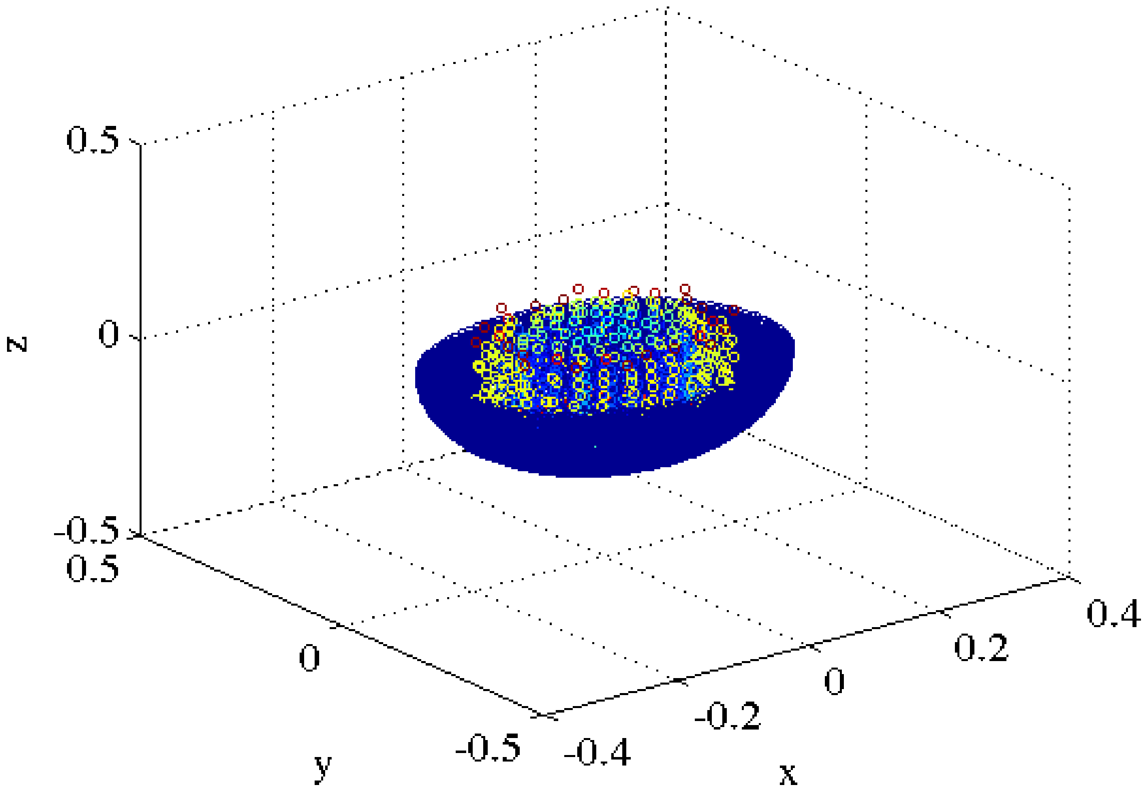

Preliminary results

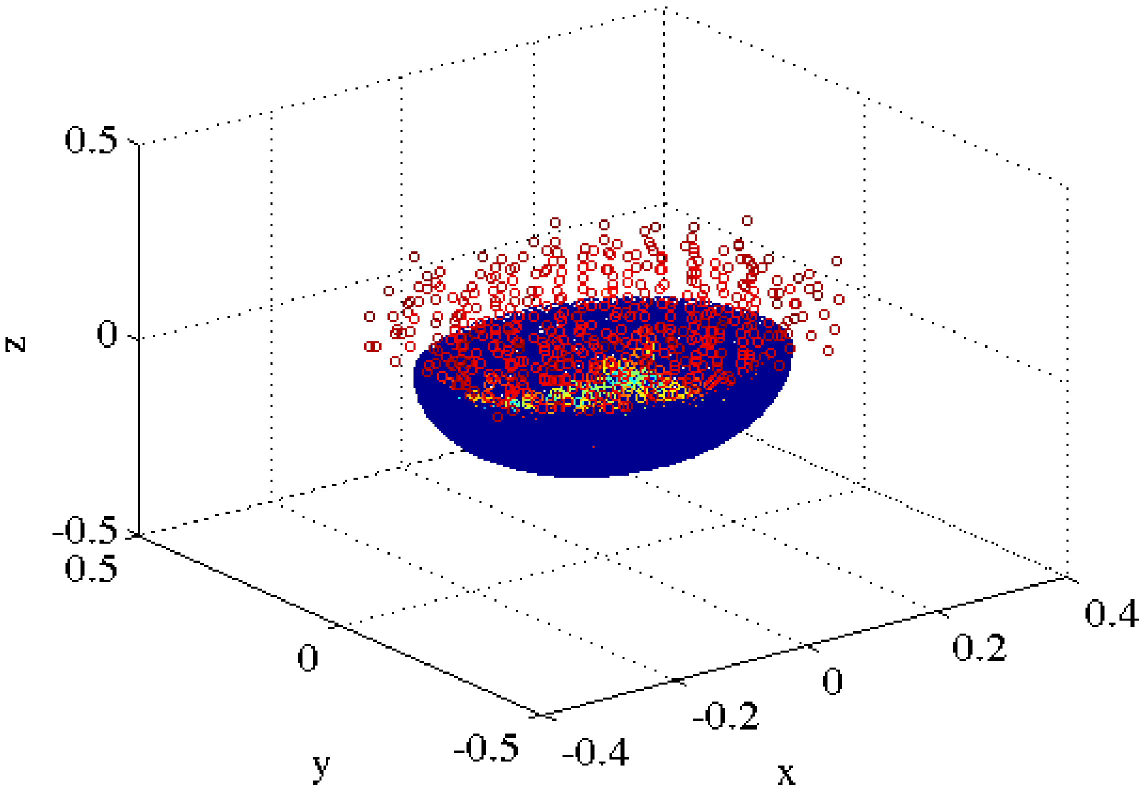

Preliminary results

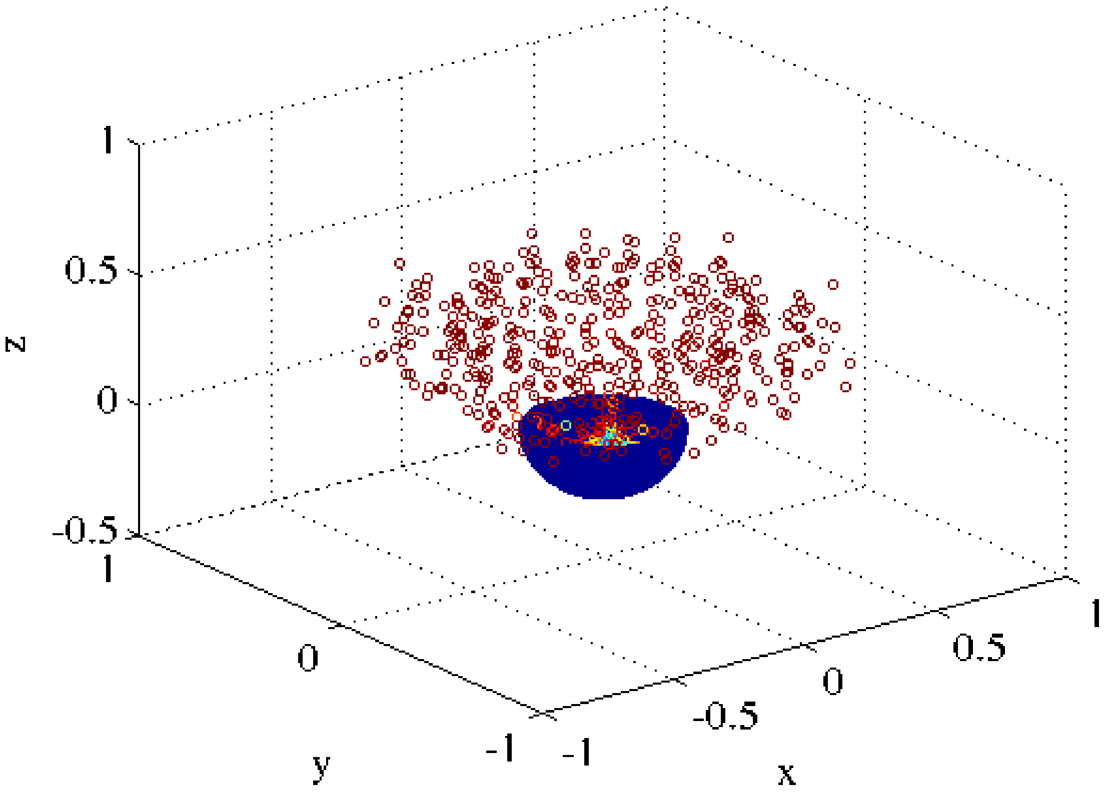

NIAC Phase I Goals

Crewed Mars Mission Concept

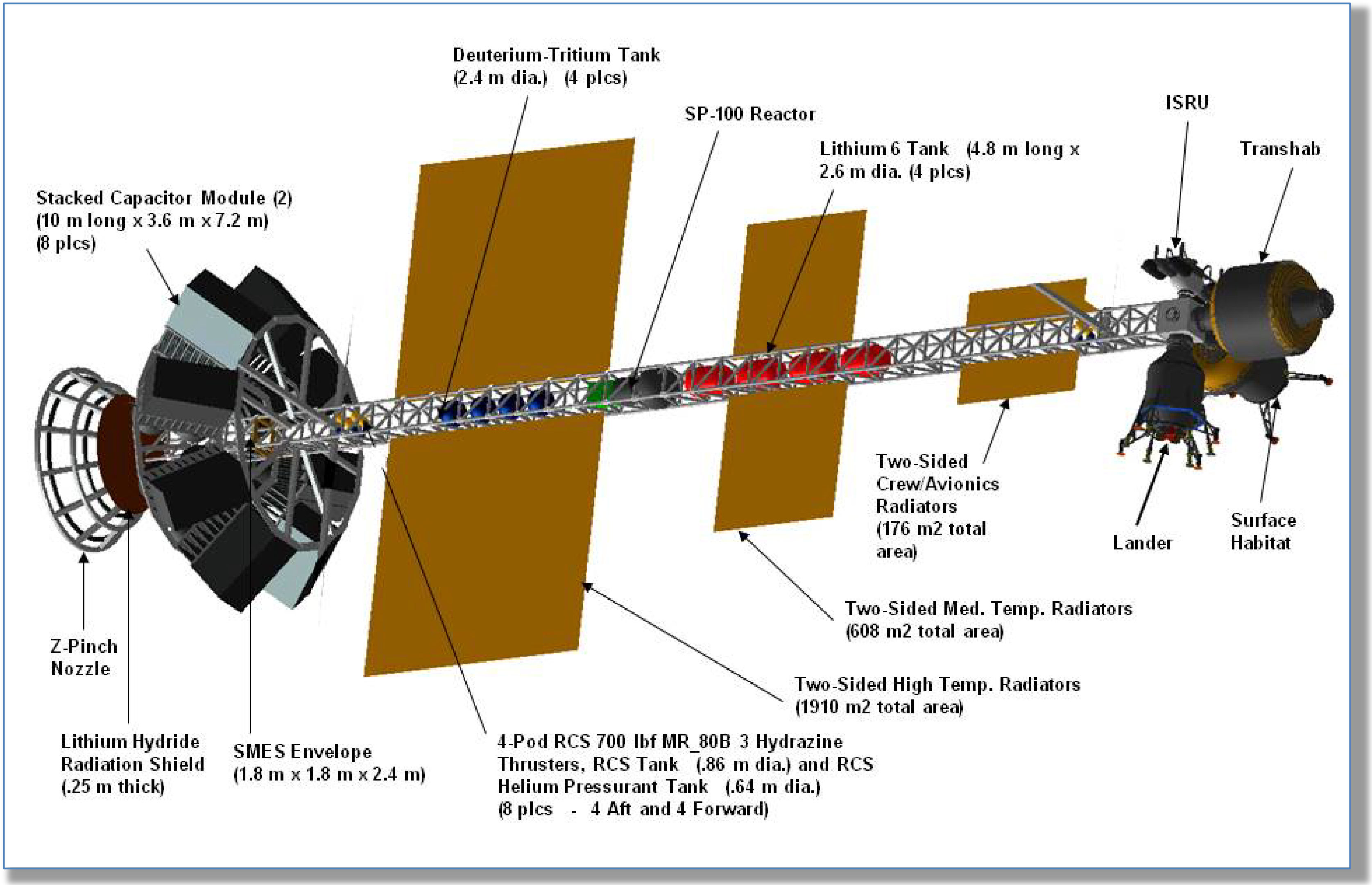

Polsgrove, T. et al. Design of Z-Pinch and Dense Plasma Focus Powered Vehicles, 2010 AIAA Aerospace Sciences Meeting

Mission Concepts

	Mars 90	Mars 30	Jupiter	550 AU
Outbound Trip Time (days)	90.2	39.5	456.8	12936
Return Trip Time (days)	87.4	33.1	521.8	n/a
Total Burn Time (days)	5.0	20.2	6.7	11.2
Propellant Burned (mT)	86.3	350.4	115.7	194.4
Equivalent DV (km/s)	27.5	93.2	36.1	57.2

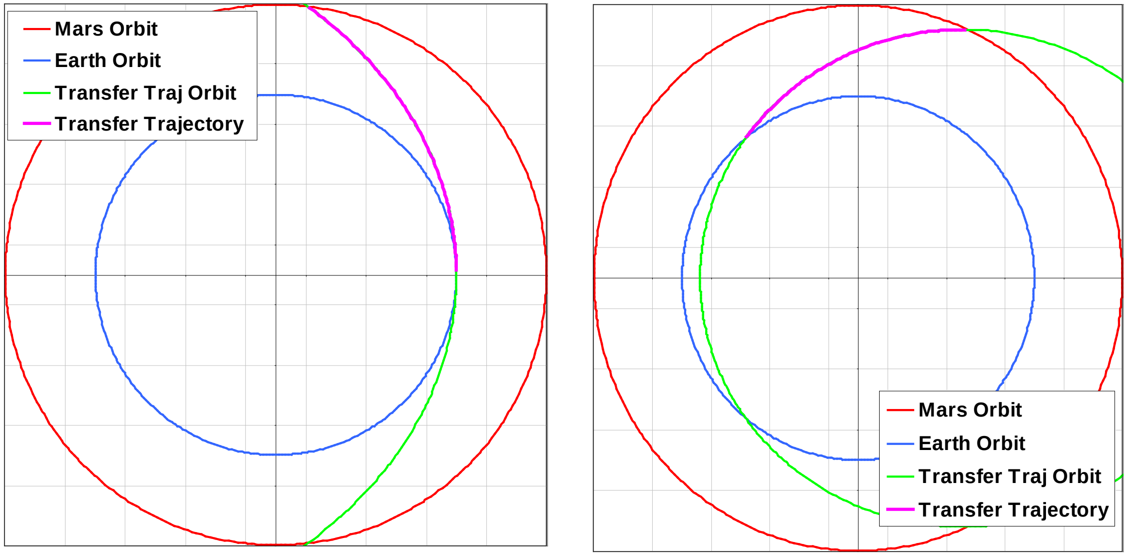

Figure 3 Mars 90 Day Transfer Trajectories

- **Engine**
    - Isp = 19,400 sec
    - T = 38 kN
    - 10 Hz pulse freq.
- **Vehicle**
    - M_{dry} = 552 mT
    - M_{pay} = 150 mT
    - 30% MGA

Polsgrove, T. et al. Design of Z-Pinch and Dense Plasma Focus Powered Vehicles, 2010 AIAA Aerospace Sciences Meeting

Mating SPFMaX and MCNP

- **SPFMax gives**
  - Ability to model 3d effects
  - Can propagate magnetic fields in vacuum
  - Easily editable
- **MCNP**
  - Track neutron life, fission reactions
  - Flexible geometries
- **Second half of NIAC is to run codes concurrently**
  - synchronize neutron population vs. time
  - Optimize energy output
    - As function of geometry
    - As function of composition
      - Mix of UF6, D-T
      - Lithium liner thicknesses

Single turn Magnetic Nozzle

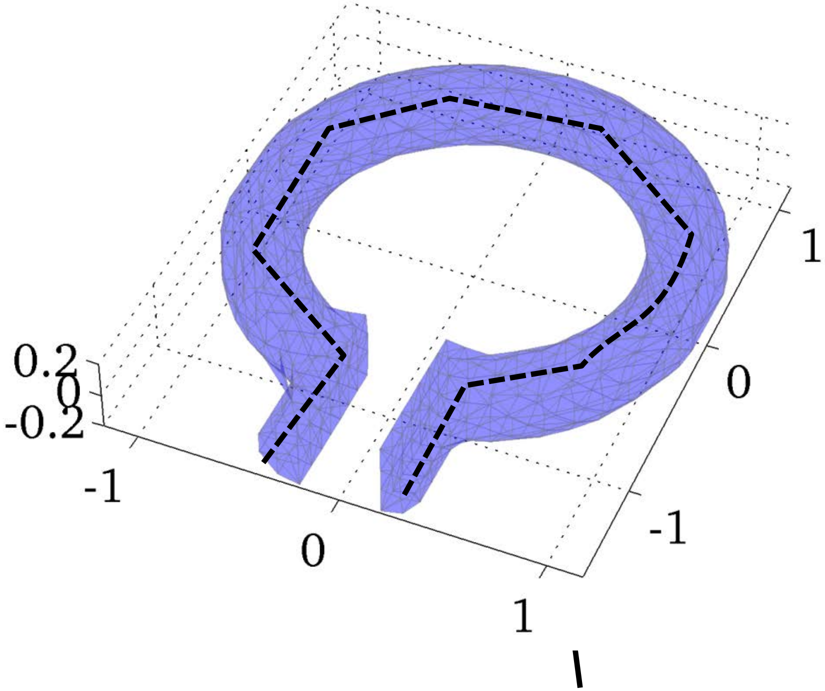

Direction of current

- Gasdynamic nozzle performance to be compared with magnetic nozzle to assess loss mechanisms in magnetic nozzles, e.g.
  - Field/plasma instabilities
  - Plasma detachment

Charger - 1

- A test facility for high power and thermonuclear fusion propulsion concepts, astrophysics modeling, radiation physics
- Located in the UAH Aerophysics Lab at Redstone
- The highest instantaneous pulsed power facility in academia – 572 kJ (1 TW at 100 ns)

Long Range Plans

- **NIAC Phase II**
  - Complete Charger 1 refurb
  - Ignite PuFF plasma
  - Continue magnetic nozzle research
- **Charger II**
  - Construct breadboard PuFF system capable of 10-20 Hz operation
    - Upgrade to flight weight hardware – NASA
    - Optimize pulse for maximum power output – DOE
    - Astrodynamics, radiation protection, other research goals - Various